Supporting Information: Enhancing acid gas separations using free volume manipulation for microporous poly(arylene ether)s

Taigyu Joo,[a,1] Yifan Wu,[b,1] Tae Hoon Lee,[a] Pablo A. Dean,[a] Wan-Ni Wu,[a] Timothy M. Swager,[b] and Zachary P. Smith[a,*]

[a] Department of Chemical Engineering, Massachusetts Institute of Technology, Cambridge, MA 02139, United States

[b] Department of Chemistry, Massachusetts Institute of Technology, Cambridge, MA 02139, United States

[1] The authors contributed equally to this work.

* Corresponding Author. Email address: zpsmith@mit.edu; Postal address: Massachusetts Institute of Technology, Department of Chemical Engineering, 77 Massachusetts Avenue, Room 66-466, Cambridge, MA, USA 02139-4307

Table of Contents

1. Materials and polymer synthesis

1.1. Materials

All reagents used in this paper were purchased from commercial sources (Sigma-Aldrich, Ambeed) and used as received. He (HE UHP300, 99.999%), H_2 (HY UHP300, 99.999%), CH_4 (ME UHP300, 99.99%), N_2 (NI UHP300, 99.999%), O_2 (OX UHP300, 99.994%), CO_2 (CD UP300, 99.995%), H_2S (air certified standard mixture, 99.99%), and 3% O_2/balance N_2 (XO2N97C3005769) were purchased from Airgas.

1.2. PAE-Cl synthesis

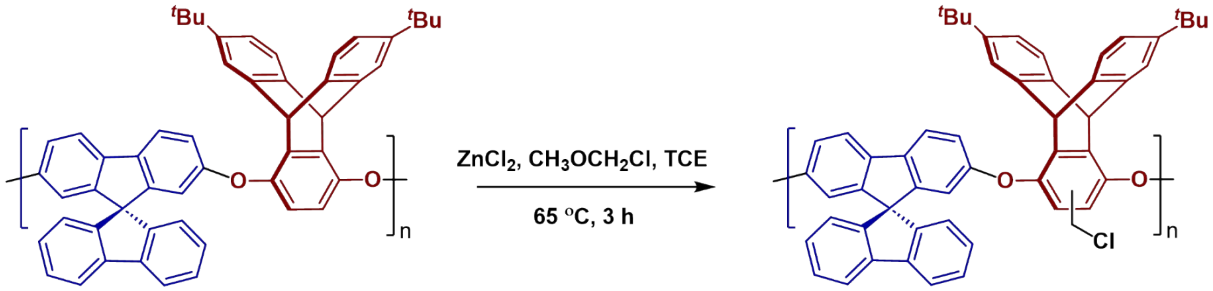

PAE-1 PAE-Cl

The polymer starting material was synthesized following a procedure described in our previous study.[1,2] To a 100 mL three-necked flask equipped with a stir bar, a nitrogen inlet, and a condenser, PAE-1 (710 mg, 1 mmol) and anhydrous zinc chloride (0.41 g, 3.0 mmol) were added. The flask was evacuated and backfilled with nitrogen from the Schlenk line (this process was repeated a total of three times). Then, tetrachloroethane (TCE, 23.6 mL) was added, and the mixture was stirred adequately to form a homogeneous solution. Chloromethyl methyl ether (0.61 mL, 8 mmol) was added dropwise to the solution. The resulting solution was heated to 65 °C for 3 h. After that, the mixture was cooled to room temperature and precipitated in methanol with vigorous stirring. The resulting fiber-like polymer was washed with methanol several times and dried under vacuum for 24 h at 120 °C before used. The product PAE-Cl was collected as a white-

solid (698 mg, 92% yield) after precipitation. ^{1}H NMR (500 MHz, $CDCl_3$): δ 7.85–6.12 (m, 21H), 5.77–5.45 (m, 2H), 4.70 (m, 2H), 1.21 (s, 18H).

1.3. PAE-PIP-tBOC synthesis

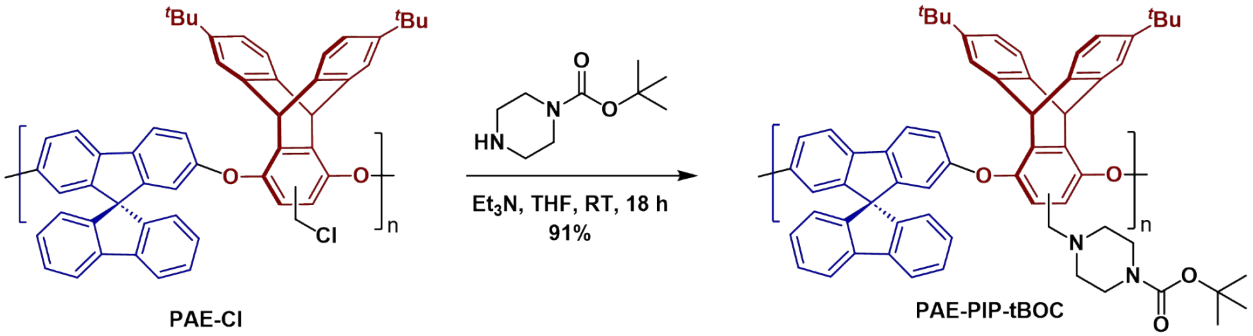

To a 50 mL round-bottom flask equipped with a stir bar, PAE-Cl (698 mg, 0.92 mmol) and THF (5 mL) were added. The mixture was stirred adequately to form a homogeneous solution. Triethylamine (Et_3N, 1.3 mL, 9 mmol) and 1-BOC-piperazine (1.86 g, 10 mmol) were added dropwise to the solution. The mixture was stirred overnight and precipitated in methanol twice. The resulting product PAE-PIP-tBOC was dried under vacuum for 24 h before used. ^{1}H NMR (500 MHz, $CDCl_3$): δ 7.25–7.87 (m, 6H), 6.23–7.13 (m, 12H), 5.35–5.89 (m, 2H), 3.20–3.48 (m, 6H), 2.37 (m, 4H), 1.45–1.47 (m, 9H), 1.18–1.20 (m, 18H).

2. Additional characterization – experimental procedures

2.1. Density Measurements

The density of the polymer samples was determined based on Archimedes' principle using a Mettler Toledo density measurement kit (ME-DNY-4, Switzerland). The density of each sample was calculated using the following equation:

$$\rho = \frac{M_{air}\rho_{sol}}{M_{air} - M_{sol}} \#(S1)$$

where M_{air} is the mass of the polymer film measured in air, M_{sol} is the mass of the polymer film when immersed in a reference solvent, and ρ_{sol} is the density of the reference solvent. Hexadecane at room temperature was used as the reference solvent. To ensure accuracy and reproducibility, the density of each polymer sample was determined using at least four separate pieces of polymer film. The uncertainty in the reported density values is expressed as the standard deviation derived from these multiple measurements.

2.2. Proton nuclear magnetic resonance spectroscopy (^{1}H NMR)

^{1}H NMR spectra were recorded on a Bruker 500 MHz spectrometer, and ^{1}H spectrum was calibrated using residual solvent as an internal reference ($CHCl_3$: δ 7.26 ppm). The following abbreviations were used to denote multiplicities: s = singlet, bs = broad singlet, d = doublet, t = triplet, q = quartet, m = multiplet.

2.3. Thermal gravimetric analysis with mass spectroscopy (TGA-MS)

Thermogravimetric analysis coupled with mass spectrometry (TGA-MS) was conducted using a TA Instruments 5500 Thermogravimetric Analyzer (USA) connected to a ThermoStar® GSD 350T Mass Spectrometer (Pfeiffer Vacuum, Germany). The isothermal heating protocol, as outlined in *Section 2.2* of the main article, was followed to replicate the FVM process, with in-

house N_2 or air supplied to the TGA chamber. The mass spectrometer operated over a scan range of 1–80 m/z to capture a wide range of potential molecular fragments produced during the FVM process. The ion current for each detected m/z value was summed and normalized to the highest observed intensity, allowing for the relative abundance of all scanned m/z species to be plotted over the entire FVM process.

2.4. X-ray photoelectron spectroscopy (XPS)

To investigate the surface chemistry and elemental composition of the polymer samples, X-ray photoelectron spectroscopy (XPS) was conducted using PHI VersaProbe II (ULVAC-PHI Inc., Japan) equipped with an Al-Kα radiation source (hν = 1486.6 eV).

2.5. Wide-angle X-ray scattering (WAXS)

Wide-angle X-ray scattering (WAXS) patterns were collected using a SAXSLAB machine (Denmark) equipped with a DECTRIS PILATUS3 R 300K detector and Rigaku 002 microfocus X-ray source. The scattering data for each sample was collected for 1,200 s under approximately 0.08 mbar. The obtained patterns were analyzed and plotted as intensity $I(q)$ versus the scattering wavevector q, calculated as follows:

$$q = \frac{4\pi \sin\theta}{\lambda} \#(S2)$$

where θ is the Bragg angle and λ is the wavelength of the X-ray beam. The peaks identified in these WAXS patterns were analyzed and fitted using a "gaussian peak + slope background" model from the SAXSGUI software program.

2.6. Brunauer-Emmett-Teller (BET) measurements

Physisorption isotherms of the polymer film samples were obtained with the Brunauer-Emmett-Teller (BET) technique using a Micromeritics 3Flex instrument (USA). For these

measurements, polymer film samples of at least 0.1 g were placed in pre-weighed BET tubes, and the samples were degassed for 12 hours at 120 °C using a Micromeritics Smart VacPrep system (USA). The sorption uptake of CO_2 was recorded at 273 K and 298 K over a pressure range of 0.5–760 mmHg. The apparent surface areas of the polymer films were calculated using the BET method in the relative pressure (P/P_o) range of 0.004–0.012. For a more detailed analysis of pore size distribution, non-localized density functional theory (NLDFT) was applied. Additionally, the isosteric heat of sorption for CO_2 was calculated from the sorption data using the Clausius-Clapeyron equation at 273 K and 298 K.

3. Additional characterization – results

Table S1. A summary of the samples in this work, including the number of samples tested, thickness, density, and fractional free volume (FFV) calculated from the updated group contribution theory by Wu et al.[3] All uncertainties are noted as standard deviations.

Polymer	**# of samples**	**Thickness** (μm)	**Density** (g/cm^3)	**FFV**[c]
PAE-1[a]	5	64.7 ± 3.2	1.09 ± 0.01	0.21 ± 0.01
PAE-PIP-tBOC[b]	1	50.0 ± 14.1	1.06 ± 0.01	0.22 ± 0.01
PAE-PIP-FVM-0[a]	3	57.2 ± 11.1	1.06 ± 0.02	0.23 ± 0.02
PAE-PIP-FVM-3[a]	5	68.0 ± 12.0	1.20 ± 0.02	–
PAE-1-3[b]	1	81.4 ± 2.5	–	–

[a]The presented value is an average of all samples, and the errors indicate standard deviations from multiple samples.
[b]The presented value is for one sample, and the errors indicate standard deviations of multiple measurements.
[c]The calculation of FFV for PAE-PIP-FVM-3 using group contribution theory is challenging due to the difficulty in determining the exact chemical structure and the extent of crosslinking.

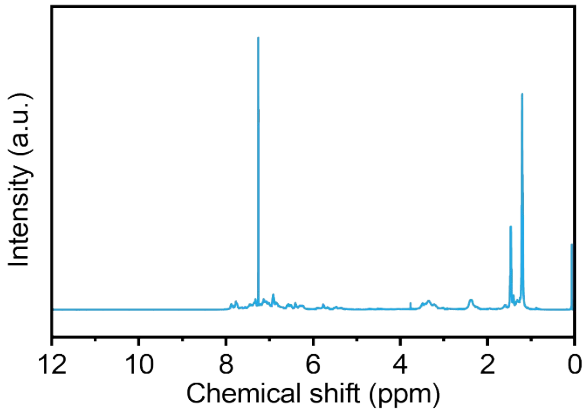

Figure S1. ^{1}H NMR spectra of PAE-PIP-tBOC.

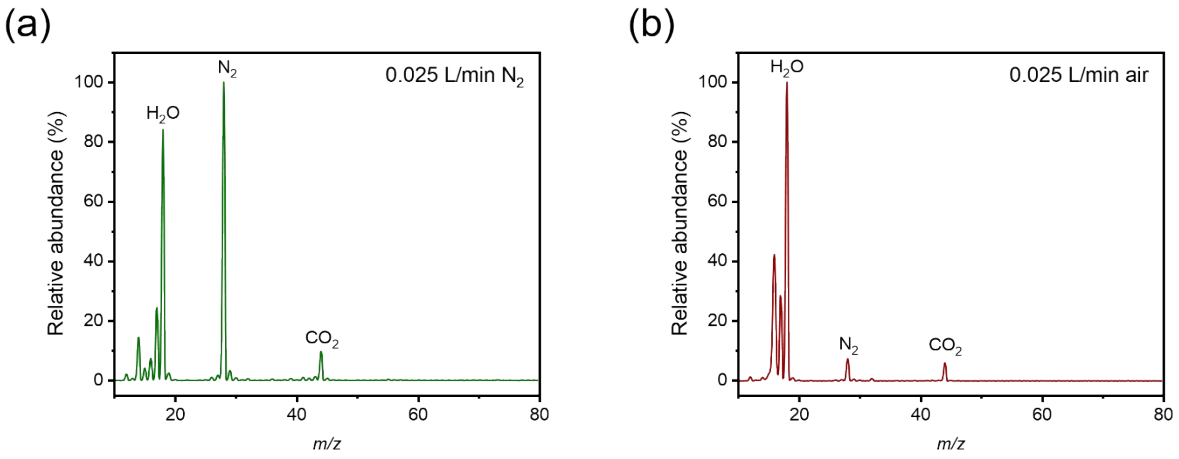

Figure S2. Mass spectra of evolved gases from thermally treating PAE-PIP-tBOC film during an isothermal hold at 300 °C for 16 h, replicating the FVM process under (a) N_2 and (b) air. The ion current for each m/z throughout the entire isothermal hold was summed and normalized to the highest observed intensity.

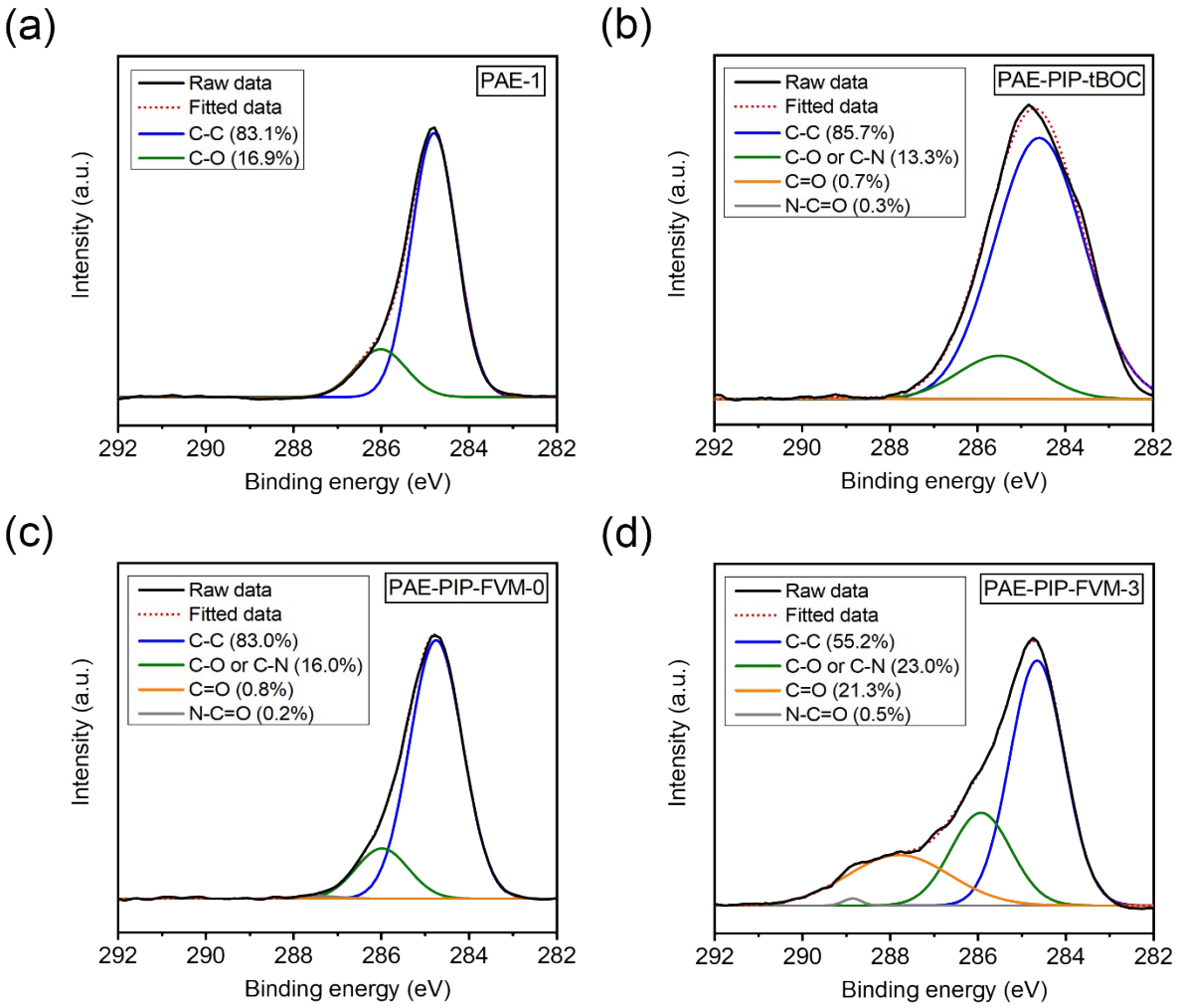

Figure S3. XPS spectra of (a) PAE-1, (b) PAE-PIP-tBOC, (c) PAE-PIP-FVM-0, and (d) PAE-PIP-FVM-3.

Table S2. Surface atomic concentrations for all polymers obtained from XPS.

Polymer	at.% C1s	at.% N1s	at.% O1s
PAE-1	88.29	0.28	11.43
PAE-PIP-tBOC	88.82	2.72	8.46
PAE-PIP-FVM-0	89.56	2.38	8.06
PAE-PIP-FVM-3	70.01	9.01	20.98

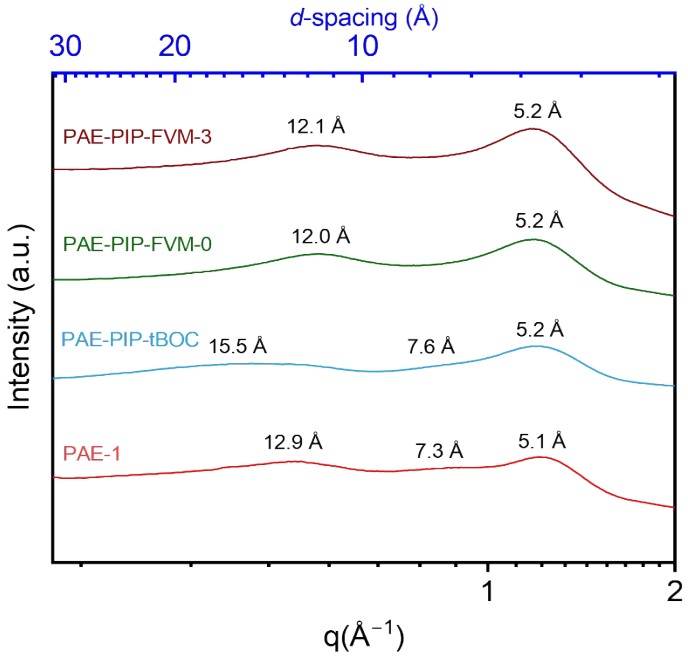

Figure S4. Comparison of WAXS scattering patterns for PAE films that have undergone FVM.

Table S3. *d*-spacing calculated from the WAXS patterns.

Polymer	***d*-spacing** (Å)		
	P1	P2	P3
PAE-1	5.1	7.3	12.9
PAE-PIP-tBOC	5.2	7.6	15.5
PAE-PIP-FVM-0	5.2	-	12.0
PAE-PIP-FVM-3	5.2	-	12.1

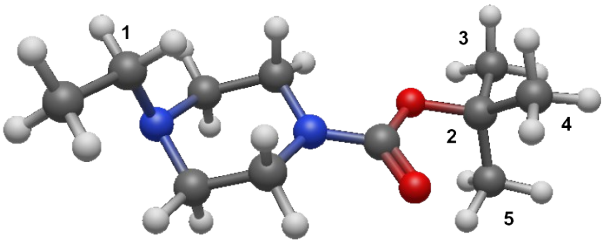

Carbon	Distance (A)
1 to 2	7.14
1 to 3	7.92
1 to 4	7.61
1 to 5	7.86
Average	7.63
St. Dev.	0.31

Figure S5. Image of a simplified structural analogue of PAE-PIP-tBOC and a tabulated C–C distances.

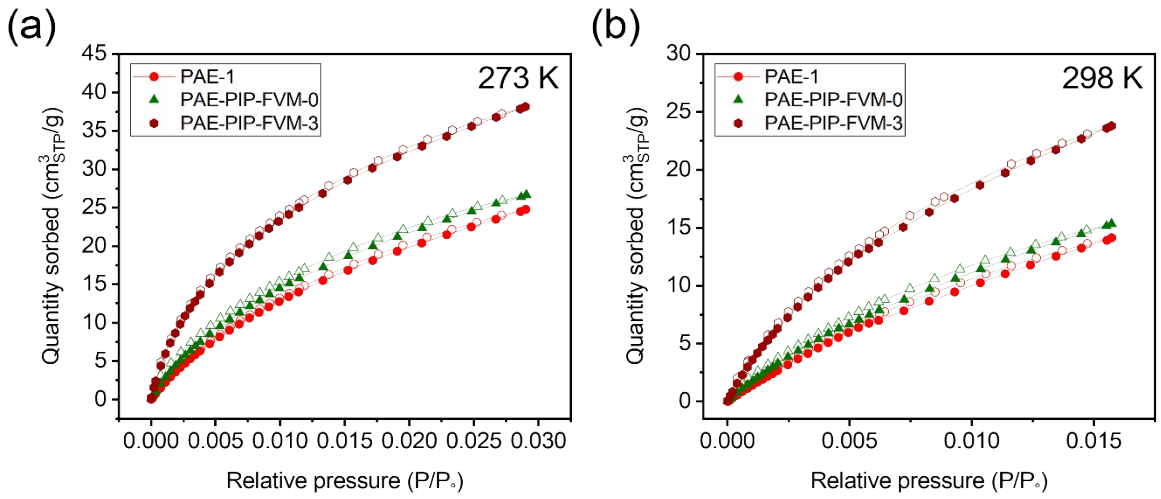

Figure S6. Comparison of CO_2 sorption at (a) 273 K and (b) 298 K for PAE-1, PAE-PIP-FVM-0, and PAE-PIP-FVM-3 films. Filled and unfilled symbols correspond to sorption and desorption steps, respectively.

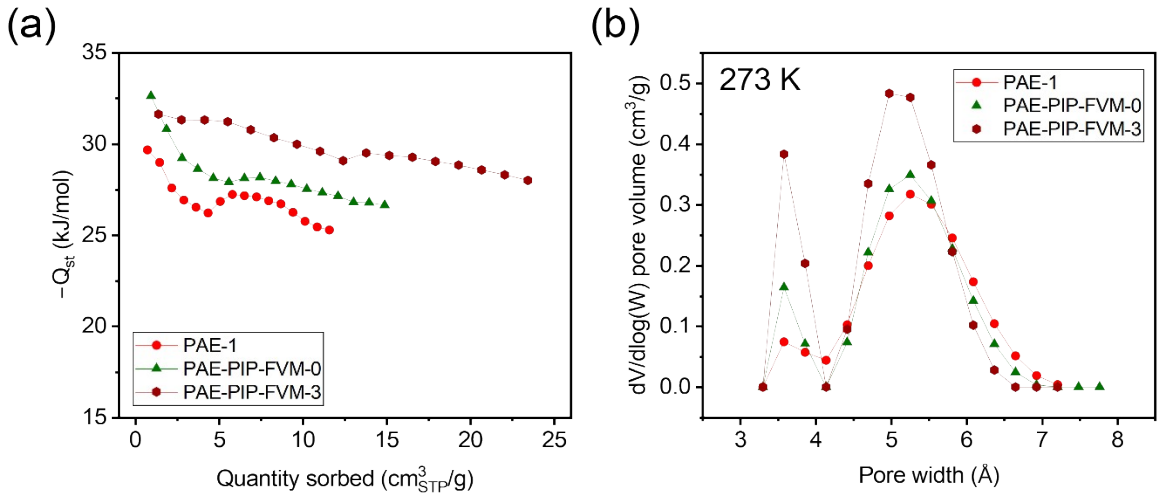

Figure S7. Comparison of (a) isosteric heat of sorption ($-Q_{st}$) and (b) pore volume distribution calculated using nonlocal density functional theory (NLDFT) for PAE-1, PAE-PIP-FVM-0, and PAE-PIP-FVM-3 films.

Table S4. Comparison of BET surface area (SA) for film samples at 273 K and 298 K and average isosteric heat of sorption ($-Q_{st}$).

Polymer	**BET SA at 273 K** ($m^2\ g^{-1}$)	**BET SA at 298 K** ($m^2\ g^{-1}$)	**Average** $-Q_{st}$ ($kJ\ mol^{-1}$)
PAE-1	132.9 ± 1.7	112.9 ± 3.5	26.9 ± 1.1
PAE-PIP-FVM-0	132.4 ± 2.5	119.2 ± 3.8	28.2 ± 1.5
PAE-PIP-FVM-3	161.3 ± 2.1	140.2 ± 2.7	29.9 ± 1.0

4. Gas transport experiments – pure gas

Table S5. Average gas permeability of tested gases measured at 15 psia (1 atm) and 35 °C. The errors are standard deviations unless noted otherwise.

Polymer	**Permeability** (barrer)						
	He	H_2	O_2	N_2	CH_4	CO_2	H_2S[a]
PAE-1	188 ± 11	344 ± 24	66.7 ± 6.4	15.4 ± 1.4	25.9 ± 2.4	324 ± 30	151 ± 3
PAE-PIP-tBOC[a]	49.7 ± 1.1	78.1 ± 1.7	9.89 ± 0.22	1.75 ± 0.04	2.74 ± 0.05	45.7 ± 0.9	–
PAE-PIP-FVM-0	124 ± 7	207 ± 19	35.9 ± 4.7	8.10 ± 1.41	13.8 ± 2.3	170 ± 26	85.7 ± 1.3
PAE-PIP-FVM-3	277 ± 88	477 ± 168	76.2 ± 34.8	17.0 ± 10.3	17.2 ± 11.1	376 ± 153	123 ± 2
PAE-1-3[a]	181 ± 6	295 ± 9	50.8 ± 1.6	10.7 ± 0.3	16.7 ± 0.5	248 ± 8	–

[a]The presented permeability is for one sample, which was performed at 16 psia (1.1 atm). The errors are calculated from propagation of uncertainty.

Table S6. Average gas selectivity of tested gases measured at 15 psia (1 atm) and 35 °C. The errors are standard deviations unless noted otherwise.

Polymer	**Selectivity**			
	H_2/CH_4	O_2/N_2	CO_2/CH_4	H_2S/CH_4[a]
PAE-1	13.3 ± 0.6	4.32 ± 0.07	12.5 ± 0.3	7.86 ± 0.21
PAE-PIP-tBOC[b]	28.5 ± 0.8	5.66 ± 0.17	16.7 ± 0.5	–
PAE-PIP-FVM-0	15.2 ± 1.1	4.47 ± 0.19	12.3 ± 0.2	7.92 ± 0.17
PAE-PIP-FVM-3	36.0 ± 15.3	5.09 ± 1.03	26.6 ± 8.0	8.90 ± 0.18
PAE-1-3[b]	17.7 ± 0.8	4.75 ± 0.21	14.9 ± 0.7	–

[a]The presented selectivity is for one sample, which was performed at 16 psia (1.1 atm). The errors are calculated from propagation of uncertainty.

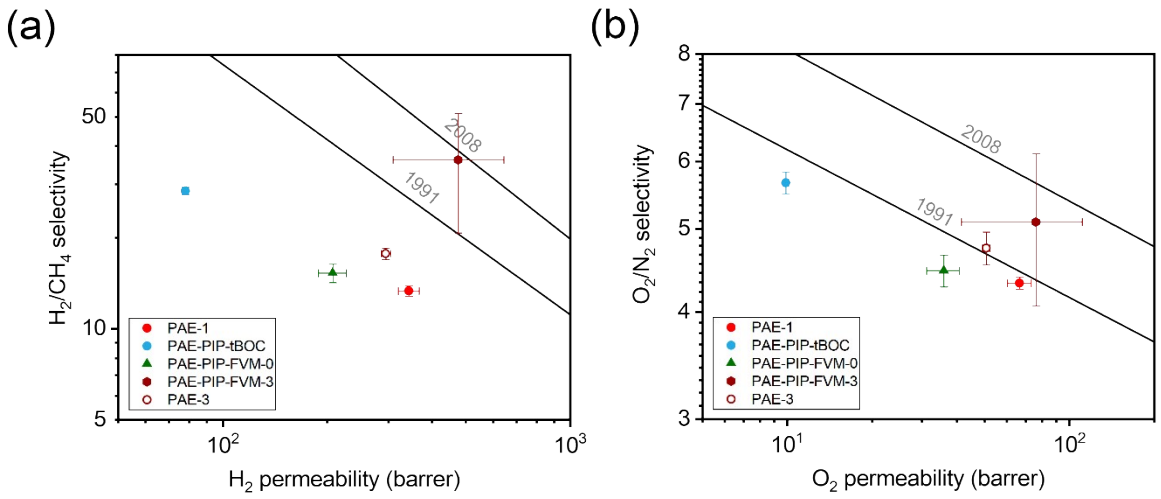

Figure S8. Pure-gas permeability and selectivity of (a) H_2/CH_4 and (b) O_2/N_2 for PAE-1 and the FVM derivatives compared with against the upper bounds.

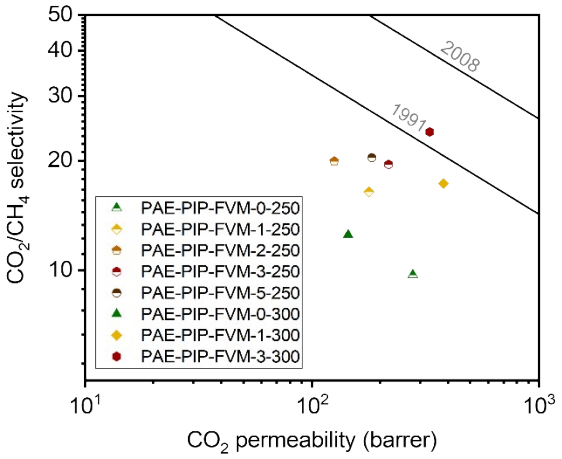

Figure S9. Pure-gas permeability and selectivity of CO_2/CH_4 for PAE-PIP-FVM samples subjected to various O_2 concentration and thermal treatment temperatures. The samples are labeled as PAE-PIP-FVM-*x*-*y*, where *x* indicates the O_2 concentration and *y* indicates the thermal treatment temperature in °C during FVM. All samples were thermally treated for 16 h.

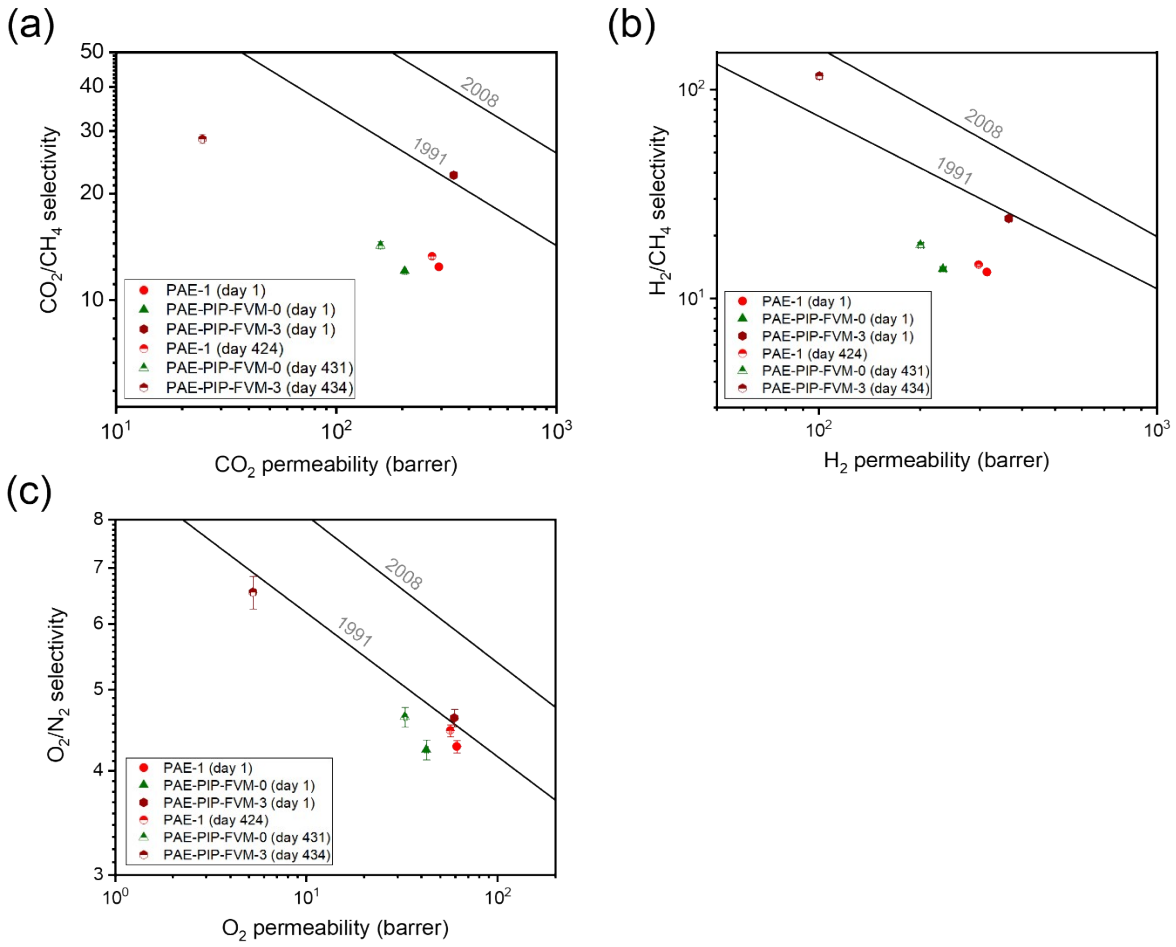

Figure S10. Pure-gas permeability and selectivity of (a) CO_2/CH_4, (b) H_2/CH_4, and (c) O_2/N_2 for PAE-1 and the FVM derivatives compared with against the upper bounds for freshly treated films (filled symbols) and aged films (half-filled symbols). Physical aging was characterized using a single film from each sample, with errors calculated through uncertainty propagation.

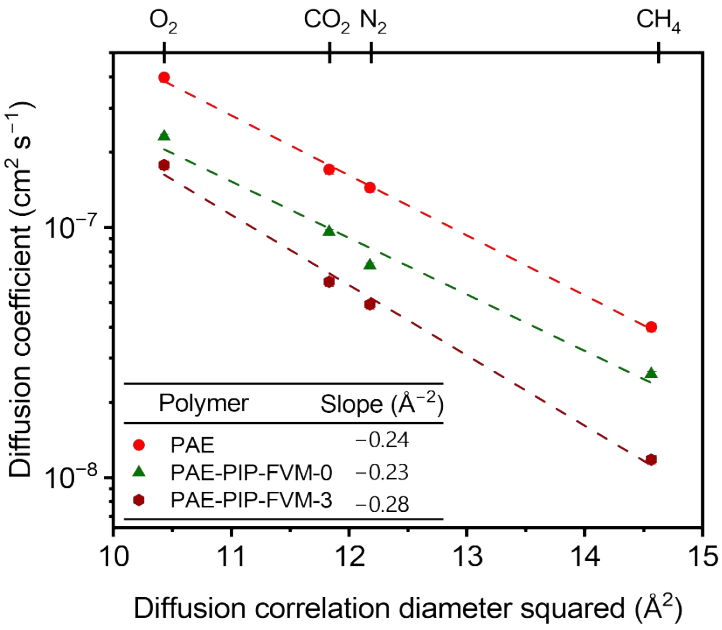

Figure S11. Comparison of diffusion coefficients obtained from time-lag method plotted against diffusion correlation diameter squared.[4] Data was fitted using an exponential model, with R^2 values exceeding 0.97 for all fits.

Table S7. Diffusion coefficients (^{D_i}) and sorption coefficients (^{S_i}) of O_2, CO_2, N_2, CH_4, and H_2S obtained from the time-lag method for the polymers studied in this work.

	Polymer	**Gas**				
		O_2	CO_2	N_2	CH_4	H_2S
D_i ($10^{-8} cm^2\ s^{-1}$)	PAE-1	39.8 ± 1.6	17.0 ± 0.7	14.4 ± 0.6	3.98 ± 0.16	2.78 ± 0.05
	PAE-PIP-FVM-0	23.0 ± 0.6	9.46 ± 0.25	6.85 ± 0.18	2.55 ± 0.07	1.46 ± 0.03
	PAE-PIP-FVM-3	17.7 ± 0.1	6.05 ± 0.26	4.91 ± 0.21	1.17 ± 0.05	1.06 ± 0.02
S_i ($cm^3_{STP}\ cm^{-3}_{pol}\ atm^{-1}$)	PAE-1	1.24 ± 0.06	13.9 ± 0.7	0.77 ± 0.04	4.54 ± 0.23	41.3 ± 1.1
	PAE-PIP-FVM-0	1.40 ± 0.05	16.3 ± 0.5	1.09 ± 0.04	4.99 ± 0.16	44.7 ± 1.1
	PAE-PIP-FVM-3	2.00 ± 0.10	30.3 ± 1.6	1.16 ± 0.06	4.08 ± 0.22	88.1 ± 2.2

The time resolution of the permeation system was inadequate for accurately determining the diffusion coefficient of H_2.

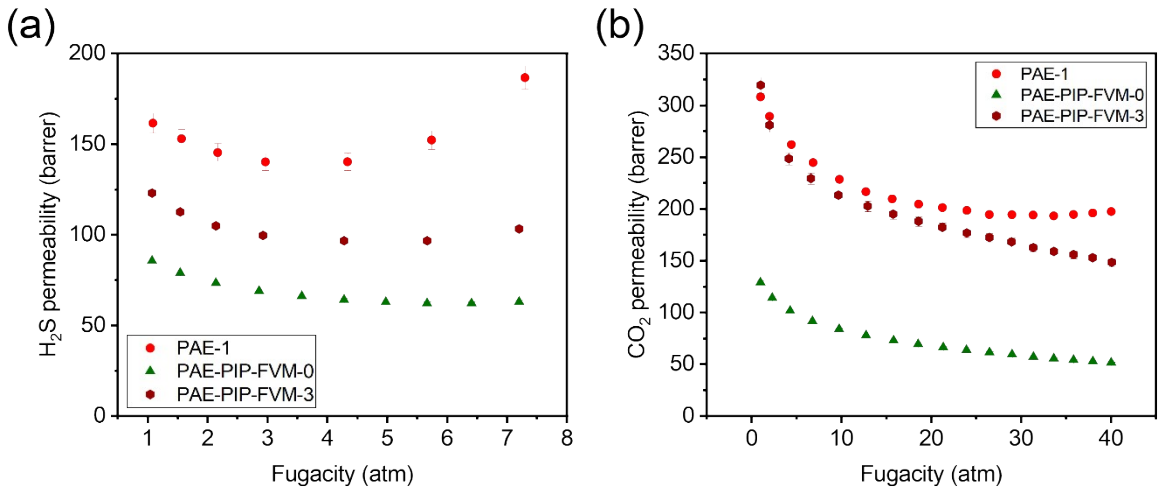

Figure S12. Comparison of permeabilities at various feed fugacities containing (a) H_2S and (b) CO_2.

Table S8. Gas permeability of tested gases for the variable-temperature study.

Polymer	Temp (°C)	Permeability (barrer)				
		H_2	O_2	CO_2	N_2	CH_4
PAE-1	35	315 ± 4	61.3 ± 0.7	293 ± 3	14.3 ± 0.2	23.6 ± 0.3
	45	330 ± 4	62.9 ± 0.8	280 ± 3	15.4 ± 0.2	25.1 ± 0.3
	55	350 ± 4	64.4 ± 0.8	264 ± 3	16.7 ± 0.2	26.8 ± 0.3
	65	371 ± 5	66.7 ± 0.8	252 ± 3	18.1 ± 0.2	28.8 ± 0.3
PAE-PIP-FVM-0	35	234 ± 5	42.5 ± 0.8	205 ± 4	10.0 ± 0.2	17.0 ± 0.3
	45	249 ± 5	44.7 ± 0.9	200 ± 4	10.8 ± 0.2	18.5 ± 0.3
	55	263 ± 5	46.6 ± 0.9	196 ± 4	12.2 ± 0.2	20.1 ± 0.4
	65	281 ± 6	48.1 ± 0.9	188 ± 4	13.6 ± 0.3	22.2 ± 0.4
PAE-PIP-FVM-3	35	682 ± 9	109 ± 1	539 ± 6	25.8 ± 0.2	28.6 ± 0.3
	45	713 ± 9	114 ± 1	531 ± 6	29.7 ± 0.3	33.9 ± 0.3
	55	743 ± 9	118 ± 1	515 ± 6	33.0 ± 0.4	38.1 ± 0.4
	65	772 ± 10	121 ± 1	488 ± 6	35.5 ± 0.4	41.9 ± 0.4

Table S9. Activation energy of permeation (E_P), activation energy of diffusion (E_D), and enthalpy of sorption (ΔH_S) for the polymers studied in this work.

	Gas	PAE-1	PAE-PIP-FVM-0	PAE-PIP-FVM-3
E_P (kJ mol^{-1})	H_2	4.7	5.3	3.6
	O_2	2.4	3.6	3.2
	CO_2	–4.4	–2.5	–2.8
	N_2	6.8	8.9	9.2
	CH_4	5.7	7.7	11.0
E_D (kJ mol^{-1})	O_2	18.8	21.7	21.4
	CO_2	18.2	19.7	21.5
	N_2	28.0	27.6	32.0
	CH_4	27.5	30.5	31.9
ΔH_S (kJ mol^{-1})	O_2	–16.4	–18.2	–18.2
	CO_2	–22.7	–22.1	–24.3
	N_2	–21.3	–18.8	–22.8
	CH_4	–21.8	–22.8	–21.0

The time resolution of the permeation system was inadequate for accurately determining the diffusion coefficient of H_2.

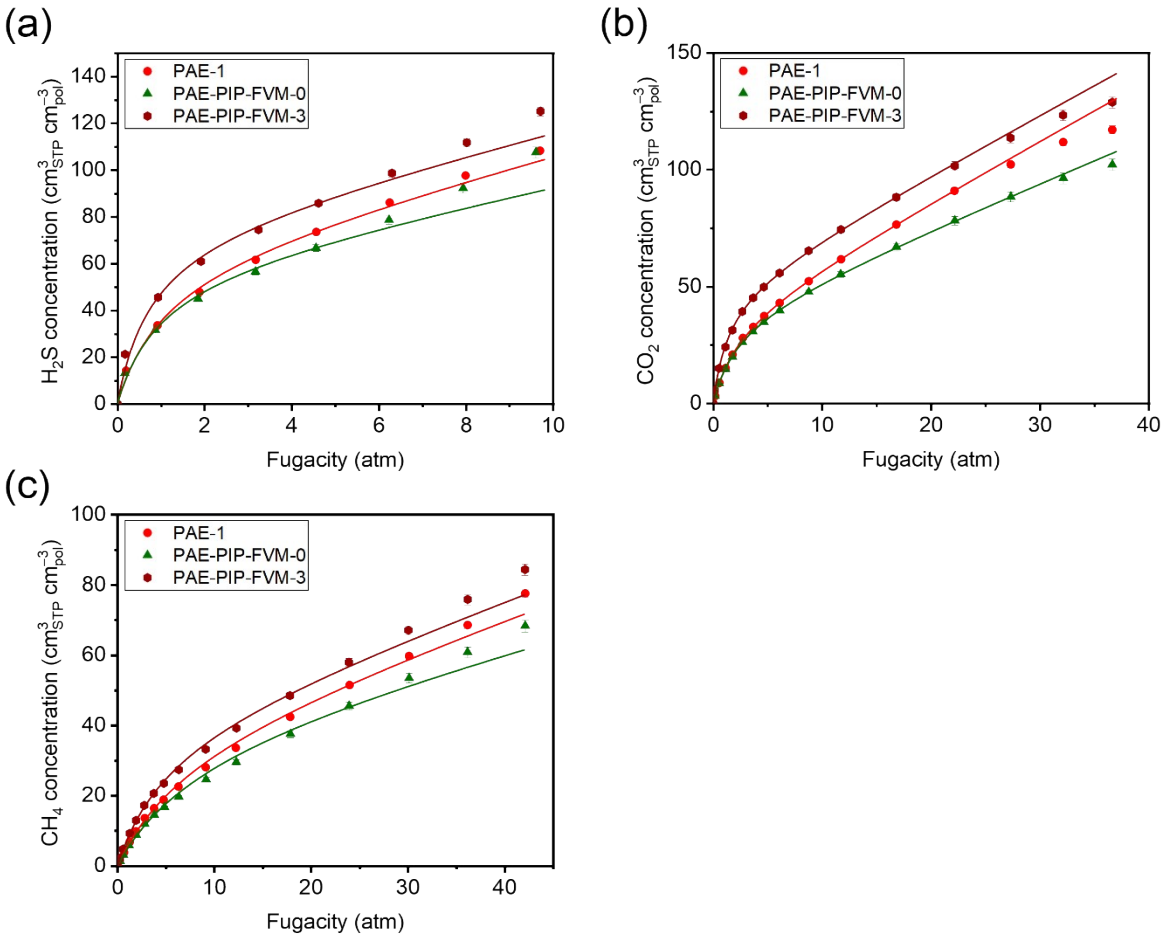

Figure S13. Sorption isotherm comparison and constrained dual-mode sorption fittings for (a) H_2S, (b) CO_2, and (c) CH_4 for fresh films of PAE-1, PAE-PIP-FVM-0, and PAE-PIP-FVM-3 measured at 35 °C. See *Section 2.5* of the main article for details on the constraints.

Table S10. Dual-mode sorption (DMS) model parameters fitted to experimental pure-gas sorption data.

Polymer	Gas	k_D $(cm^3_{STP}\, cm^{-3}_{pol}\, atm^{-1})$	$C_H^{'}$ $(cm^3_{STP}\, cm^{-3}_{pol})$	b (atm^{-1})
PAE-1	H_2S	4.74	64.6	0.898
	CO_2	2.56	38.0	0.422
	CH_4	0.93	38.3	0.131
PAE-PIP-FVM-0	H_2S	3.72	60.5	1.014
	CO_2	1.97	38.0	0.441
	CH_4	0.70	38.7	0.115
PAE-PIP-FVM-3	H_2S	4.51	76.0	1.281
	CO_2	2.51	49.8	0.699
	CH_4	0.97	41.0	0.187

5. Gas transport experiments – mixed gas

Table S11. Mixed-gas permeability and selectivity of PAE samples.

Polymer	Total pressure (atm)	Composition (%)			Permeability (barrer)			Selectivity		
		H_2S	CO_2	CH_4	H_2S	CO_2	CH_4	H_2S/CH_4	CO_2/CH_4	$(H_2S+CO_2)/CH_4$
PAE-1	2.2	0	50	50	–	247 ± 4	18.8 ± 0.3	–	13.1 ± 0.3	–
	7.8	20	20	60	145 ± 2	142 ± 2	12.0 ± 0.2	12.1 ± 0.3	11.8 ± 0.3	23.8 ± 0.5
PAE-PIP-FVM-0	2.2	0	50	50	–	144 ± 2	8.65 ± 0.12	–	16.7 ± 0.3	–
	7.8	20	20	60	67.9 ± 0.9	72.3 ± 1.0	4.74 ± 0.06	14.3 ± 0.3	15.3 ± 0.3	29.6 ± 0.5
PAE-PIP-FVM-3	2.2	0	50	50	–	346 ± 4	12.0 ± 0.2	–	28.9 ± 0.5	–
	7.8	20	20	60	126 ± 2	140 ± 2	5.56 ± 0.07	22.7 ± 0.4	25.2 ± 0.4	48.0 ± 0.7

The errors are calculated from propagation of uncertainty.

Table S12. Pure-gas permeability and selectivity of PAE samples measured at relevant mixed-gas testing pressures to compare with mixed-gas permeation results in Table S11.

Polymer	Pressure (atm)			Permeability (barrer)			Selectivity		
	H_2S	CO_2	CH_4	H_2S	CO_2	CH_4	H_2S/CH_4	CO_2/CH_4	$(H_2S+CO_2)/CH_4$
PAE-1	1.1	1.1	1.1	151 ± 3	232 ± 4	19.2 ± 0.4	7.86 ± 0.21	12.1 ± 0.3	19.9 ± 0.5
	1.6	1.6	4.7	143 ± 3	225 ± 4	18.0 ± 0.3	7.98 ± 0.22	12.5 ± 0.3	20.5 ± 0.5
PAE-PIP-FVM-0	1.1	1.1	1.1	85.7 ± 1.3	137 ± 2	10.8 ± 0.2	7.92 ± 0.17	12.6 ± 0.3	20.6 ± 0.4
	1.6	1.6	4.7	79.0 ± 1.2	129 ± 2	10.1 ± 0.2	7.85 ± 0.17	12.9 ± 0.3	20.7 ± 0.4
PAE-PIP-FVM-3	1.1	1.1	1.1	123 ± 2	331 ± 5	13.8 ± 0.2	8.90 ± 0.18	23.9 ± 0.5	32.8 ± 0.6
	1.6	1.6	4.7	113 ± 2	312 ± 4	12.8 ± 0.2	8.83 ± 0.18	24.5 ± 0.5	33.3 ± 0.6

The errors are calculated from propagation of uncertainty.

Table S13. Diffusion coefficients (D_i) and sorption coefficients (S_i) of H_2S, CO_2, and CH_4 obtained from the time-lag method for the samples in Table S12.

	Polymer	Pressure (atm)			Gas		
		H_2S	CO_2	CH_4	H_2S	CO_2	CH_4
D_i ($10^{-8} cm^2\ s^{-1}$)	PAE-1	1.1	1.1	1.1	2.78 ± 0.05	18.0 ± 0.3	3.68 ± 0.06
		1.6	1.6	4.7	4.16 ± 0.07	32.0 ± 0.5	7.33 ± 0.12
	PAE-PIP-FVM-0	1.1	1.1	1.1	1.46 ± 0.03	13.2 ± 0.3	4.29 ± 0.09
		1.6	1.6	4.7	2.18 ± 0.44	22.2 ± 0.4	6.01 ± 0.12
	PAE-PIP-FVM-3	1.1	1.1	1.1	1.06 ± 0.02	9.35 ± 0.17	1.64 ± 0.03
		1.6	1.6	4.7	1.91 ± 0.03	16.9 ± 0.3	2.26 ± 0.04
S_i ($cm^3_{STP}\ cm^{-3}_{pol}\ atm^{-1}$)	PAE-1	1.1	1.1	1.1	41.3 ± 1.1	9.82 ± 0.24	3.98 ± 0.11
		1.6	1.6	4.7	26.3 ± 0.7	5.35 ± 0.13	1.85 ± 0.04
	PAE-PIP-FVM-0	1.1	1.1	1.1	44.7 ± 1.1	7.88 ± 0.19	1.91 ± 0.05
		1.6	1.6	4.7	27.6 ± 0.7	4.43 ± 0.11	1.26 ± 0.04
	PAE-PIP-FVM-3	1.1	1.1	1.1	88.1 ± 2.2	26.8 ± 0.6	6.45 ± 0.15
		1.6	1.6	4.7	44.8 ± 1.1	14.0 ± 0.3	4.35 ± 0.10

Table S14. Pure-gas and mixed-gas permeability and selectivity of aged PAE samples under humid conditions at 50% RH and 35 °C. The pressures reported for the mixed-gas results represent the total pressure.

Polymer	Aging time (day)	Pressure (atm)	Relative humidity (%)	Composition (%)		Permeability (barrer)		Selectivity
				CO_2	CH_4	CO_2	CH_4	CO_2/CH_4
PAE-1	425	1.1	50	pure	pure	251 ± 5	18.3 ± 0.3	13.8 ± 0.3
		2.2	50	50	50	274 ± 6	15.4 ± 0.3	17.8 ± 0.5
PAE-PIP-FVM-0	435	1.1	50	pure	pure	117 ± 3	7.57 ± 0.28	15.4 ± 0.7
		2.2	50	50	50	124 ± 4	6.61 ± 0.28	20.5 ± 1.1
PAE-PIP-FVM-3[b]	438	1.1	50	pure	pure	44.4 ± 0.8	1.55 ± 0.06	28.6 ± 1.2
		2.2	50	50	50	–	–	–

[a]The errors are calculated from propagation of uncertainty.
[b]The GC peaks for the PAE-PIP-FVM-3 sample were too small to obtain reliable values.

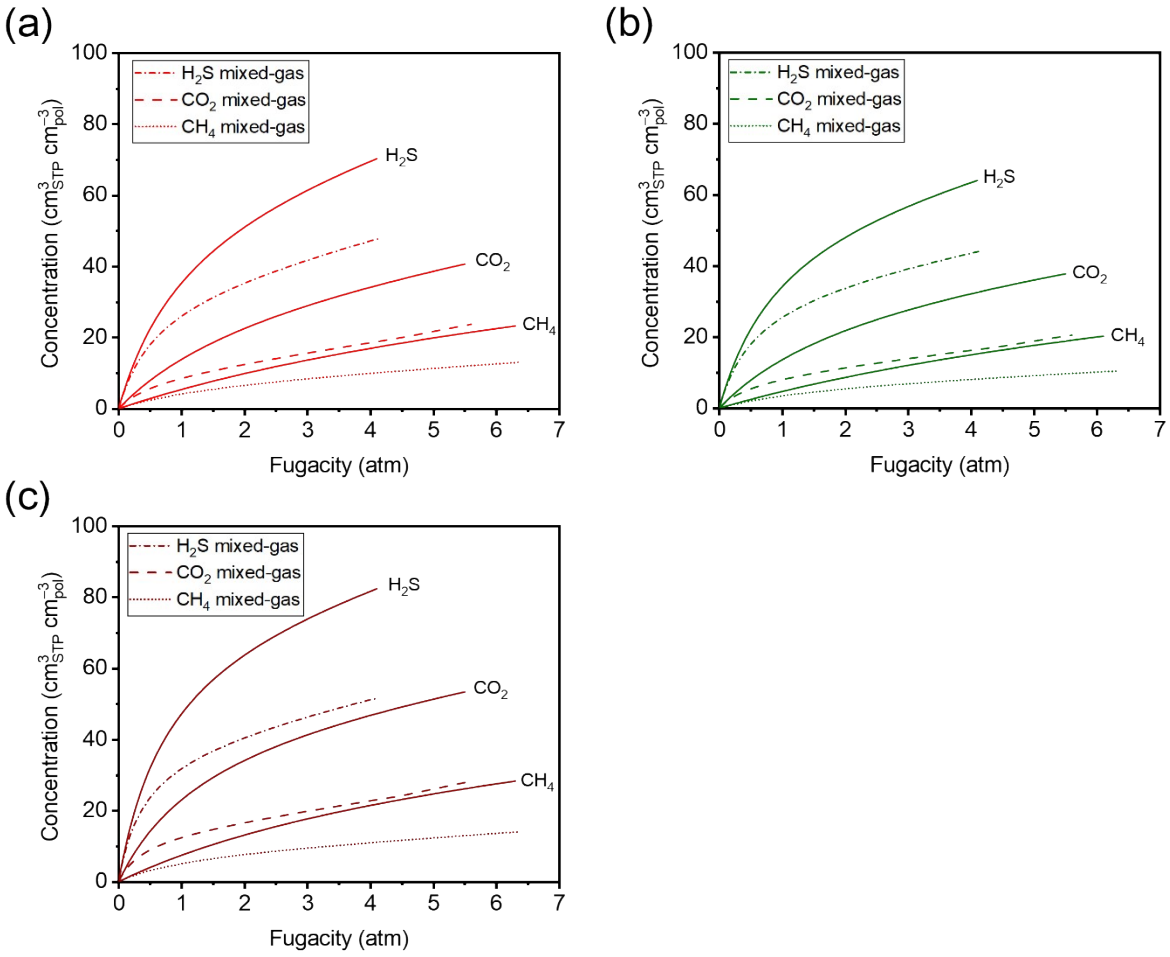

Figure S14. Comparison of experimental pure-gas isotherms (solid lines) and modeled mixed-gas sorption isotherms (dashed and dotted lines) for a 20:20:60 $H_2S/CO_2/CH_4$ mixture for (a) PAE-1, (b) PAE-PIP-FVM-0, and (c) PAE-PIP-FVM-3. The modeled isotherms are obtained from pure-gas DMS model parameters using Eqn 6 in the main text.

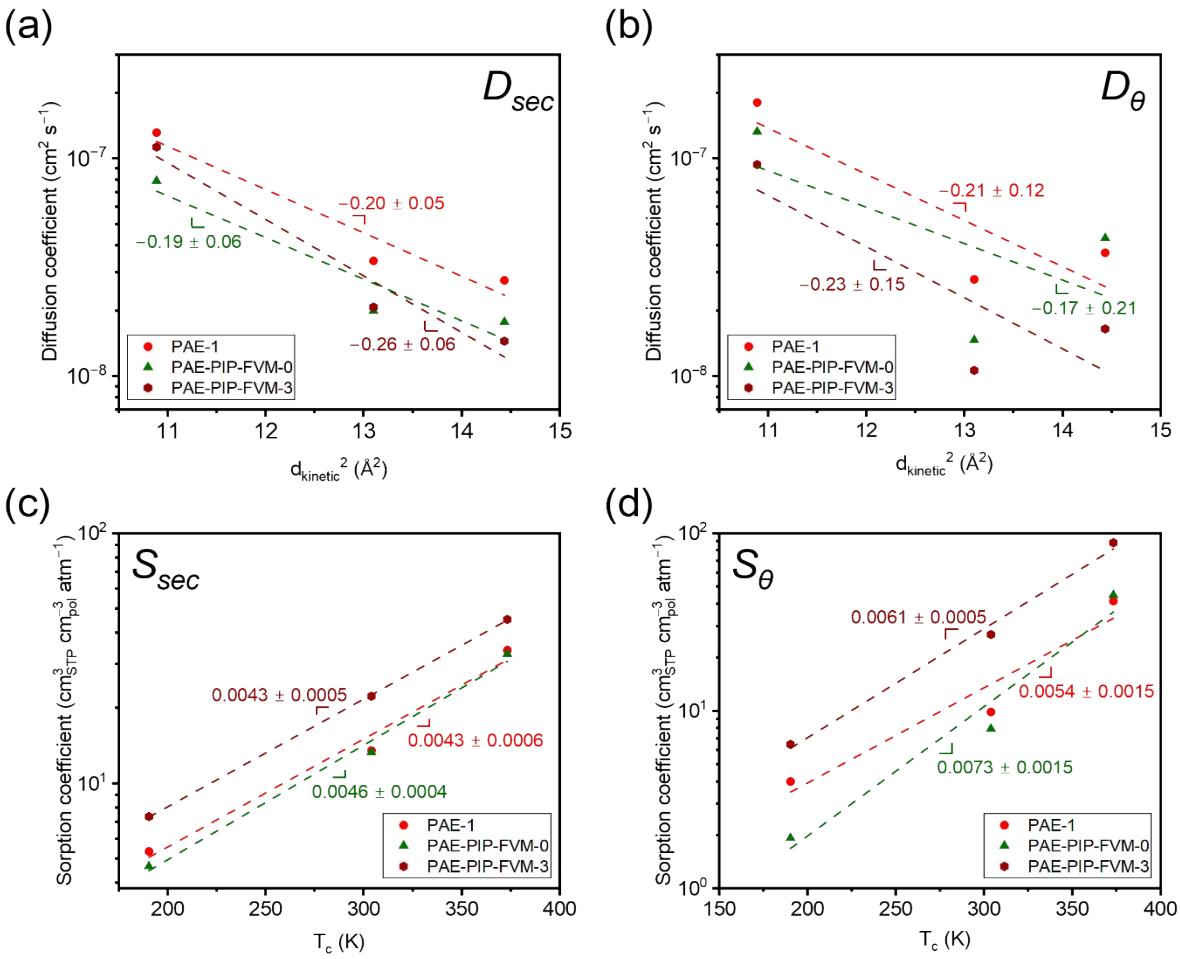

Figure S15. Diffusion coefficients of CO_2, H_2S, and CH_4 versus kinetic diameter squared ($d_{kinetic}^{\ 2}$) for PAE-1, PAE-PIP-FVM-0, and PAE-PIP-FVM-3 films, derived using (a) the secant (D_{sec}) method from the sorption isotherm data and (b) the tangent or time-lag (D_{θ}) method from the permeation data. Sorption coefficients of CO_2, H_2S, and CH_4 versus critical temperature (T_c) for PAE-1, PAE-PIP-FVM-0, and PAE-PIP-FVM-3 films, derived using (c) the secant (S_{sec}) method from the sorption isotherm data and (d) the tangent or time-lag (S_{θ}) method from the permeation data. All transport data are tested at 35 °C and 16 psia (1.1 atm).

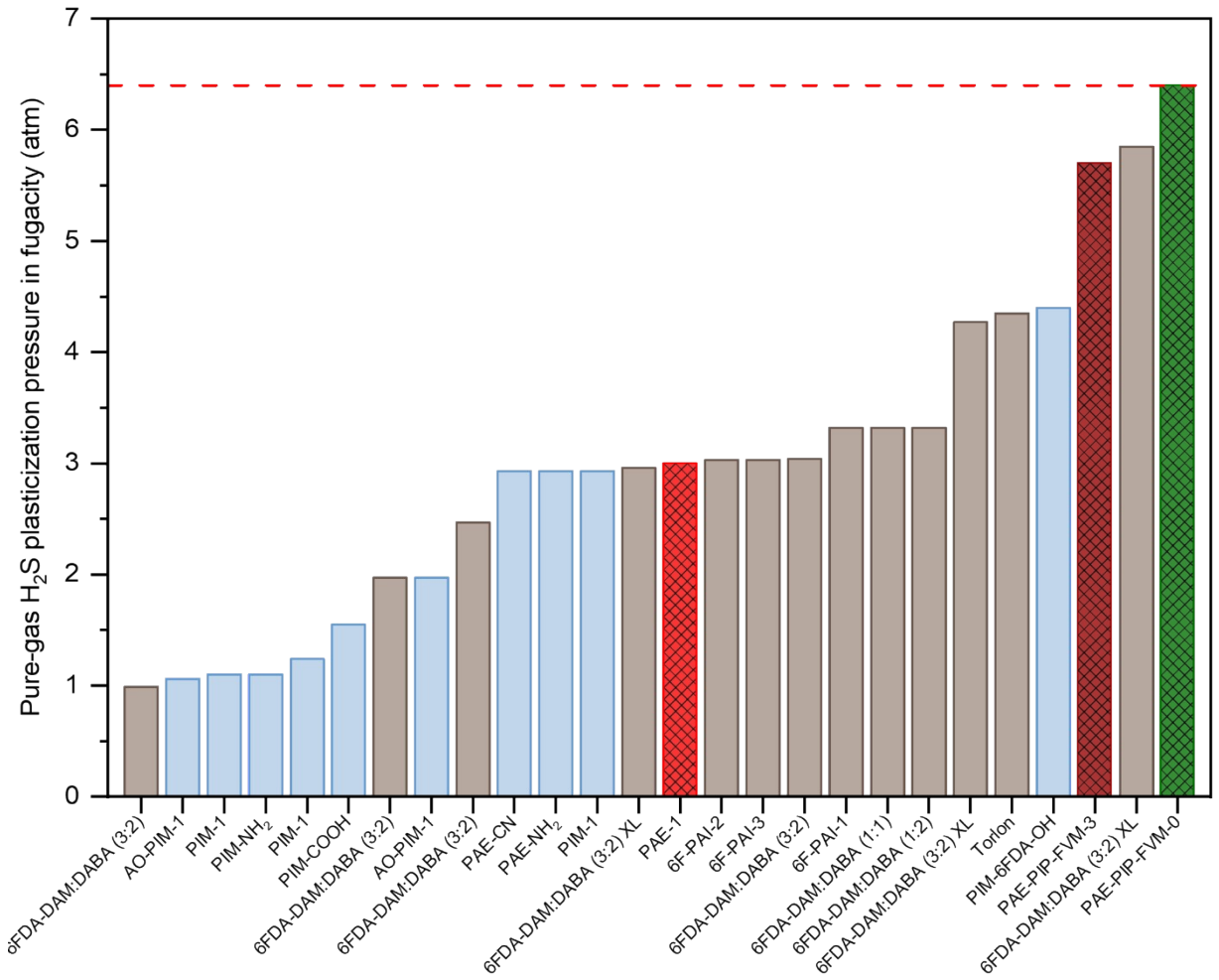

Figure S16. Comparison of pure-gas, H_2S-induced plasticization pressures for polymers from the literature[5–12] and polymers investigated in this study. The plasticization pressures were collected based on the pressure at the lowest observed permeability. Light blue colors indicate MOPs and light brown colors indicate conventional polymers. "XL" at the end of a polymer indicates a crosslinked polymer. Cross-hatched patterns indicate samples measured in this study.

6. Reference

1 S. Guo and T. M. Swager, *J. Am. Chem. Soc.*, 2021, **143**, 11828–11835.

2 P. A. Dean, Y. Wu, S. Guo, T. M. Swager and Z. P. Smith, *JACS Au*.

3 A. X. Wu, S. Lin, K. Mizrahi Rodriguez, F. M. Benedetti, T. Joo, A. F. Grosz, K. R. Storme, N. Roy, D. Syar and Z. P. Smith, *J. Membr. Sci.*, 2021, **636**, 119526.

4 L. M. Robeson, Z. P. Smith, B. D. Freeman and D. R. Paul, *J. Membr. Sci.*, 2014, **453**, 71–83.

5 B. Kraftschik, W. J. Koros, J. R. Johnson and O. Karvan, *J. Membr. Sci.*, 2013, **428**, 608–619.

6 B. Kraftschik and W. J. Koros, *Macromolecules*, 2013, **46**, 6908–6921.

7 W.-N. Wu, K. Mizrahi Rodriguez, N. Roy, J. J. Teesdale, G. Han, A. Liu and Z. P. Smith, *ACS Appl. Mater. Interfaces*, 2023, **15**, 52893–52907.

8 Z. Liu, Y. Liu, W. Qiu and W. J. Koros, *Angew. Chem. Int. Ed.*, 2020, **59**, 14877–14883.

9 S. Yi, B. Ghanem, Y. Liu, I. Pinnau and W. J. Koros, *Sci. Adv.*, 2019, **5**, eaaw5459.

10 J. Vaughn and W. J. Koros, *Macromolecules*, 2012, **45**, 7036–7049.

11 S. Yi, X. Ma, I. Pinnau and W. J. Koros, *J. Mater. Chem. A*, 2015, **3**, 22794–22806.

12 K. Mizrahi Rodriguez, P. A. Dean, S. Guo, N. Roy, T. M. Swager and Z. P. Smith, *J. Membr. Sci.*, 2024, **696**, 122464.